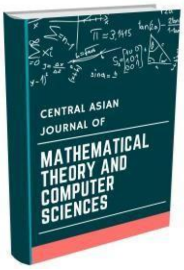

CENTRAL ASIAN JOURNAL OF MATHEMATICAL THEORY AND COMPUTER SCIENCES

https://cajmtcs.centralasianstudies.org/index.php/CAJMTCS

Volume: 06 Issue: 01 | January 2025 ISSN: 2660-5309

Article

Leveraging Probabilistic Neural Networks For Early Detection Of Respiratory Viral Infection

Abdullah Hasan Hussein

1. Department of Computer Techniques Engineering, Imam al-Kadhum College (IKC), Baghdad, 10001, Iraq

* Correspondence: Abdullahhussein87@iku.edu.iq

Abstract: The Respiratory Detection System (RDS) contributes to global mortality and necessitates suitable medical intervention. Therefore, this paper aims to classify lung MRI images into abnormal or normal categories. Our latest proposed approach involves the utilization of Probabilistic Neural Networks (PNN), incorporating both image fusion and PNN techniques. Initially, we applied several preprocessing operations, including multi-focus image fusion, to improve the exactness of MRI pictures to classify RDS. We conducted two separate experiments using distinct databases to evaluate the reliability of our PNN approach. In the first attempt, the MRI image dataset is partitioned into a 20% research set and an 80% training set, whereas in the second attempt, we employed a 10-fold cross-validation approach for the image dataset. In the first test, our methodology achieved a classification accuracy of 98.33% on dataset 1, and in the second test, it reached an accuracy of 98.77%. For dataset 2, the accuracy obtained in the first test was 92.22%, and in the second test, it was 93.33%. Hence, this control chart exhibits the potential to serve as an effective tool for the early detection of respiratory virus outbreaks, thereby facilitating prompt outbreak investigation and mitigation efforts.

Keywords: Breathing issue, Human respiratory system, Equalization, Fuzzy logic and PNN

1. Introduction

a. In-depth discussion of the importance of MRI in diagnosing and classifying RDS.
b. Concentrate on deep learning and metaheuristics methods for RDS classification via image segmentation.
c. A comparison of modern deep learning and metaheuristics approaches from 2015 to 2020

Many medical experts are applying contemporary tools to forecast RDS disorders. These strategies always assist specialists in recognizing ailments, implementing preventative measures, and facilitating treatment planning. The study of RDS diagnosis from lung MRI utilizing IP approaches is among the most common and challenging research fields. However, RDS affects a significant number of individuals regardless of their age. Identifying or predicting RDS at an early stage will save countless lives.

According to medical professionals and researchers, RDS is one of the most serious and life-threatening disorders of the human body. A late-stage RDS diagnosis is going to appear on the patient falling into a coma and in some critical cases. This leads researchers to detect and predict areas of RDS in suspicious areas with early symptoms and determine the type of RDS using lung MRI. Segmentation and IP methods are identified, and the best approach to accurately predict the location of a region in the lung using lung MRI is determined. RDS is often detected by examining serial exploratory images, and most of the time, it is primarily recognized by the symptoms of headache and other compilations.

Citation: Hussein, A. H. Leveraging Probabilistic Neural Networks For Early Detection Of Respiratory Viral Infection. Central Asian Journal of Mathematical Theory and Computer Sciences 2025, 6(1), 44-56.

Received: 01th Dec 2024
Revised: 20th Dec 2024
Accepted: 29th Dec 2024
Published: 20th Jan 2025

Medical imaging applications are continually expanding as modern technology is employed to develop disease expectations, analysis, and prevention. Annotative technology allows professionals to contribute to developing sickness diagnosis due to changes in the economy and environment. This research explores the utilizing image segmentation algorithms, a highly sought-after medical sector. However, a large number of people, regardless of age, suffer from various kinds of RDS.

Literature survey

Electrical impedance tomography [6] is an invasive estimate approach for determining Breathing Rate (BR). In any way, typical BR estimation procedures use unusual electrical sensors, and the skin contact needed by rebellious causes significant bother and annoyance to folks [7,8]. In this scenario, machine vision analysts provide non-contact BR predictions based on visual data to screen the Breathing Rate.

The technique discussed involves exploring various preprocessing methods to extract the RDS-affected region from MRI images. In the context of MRI respiratory images, it is crucial to apply smoothing and noise reduction filters. Perona and Malik's filtering approach is highlighted as particularly effective, showcasing superior results for the specific database employed in the study. Employing high-quality filters during the preprocessing step is critical because it lays the groundwork for improved results in the following phases: segmentation, classification, and picture extraction. This emphasizes the necessity of proper preprocessing techniques to maximize the overall analysis and interpretation of medical images in applications like finding RDS-affected areas in MRI scans [20].

The success of this strategy is evaluated by comparing it with other existing algorithms using performance metrics. The Fuzzy C-Means (FCM) method is highlighted for its importance in this context.

2. Materials and Methods

The approach works in two stages: first, the noisy image is filtered using a non-local principal component analysis (PCA) and then the refined image is structured into a vector image using a non-local linear filter. This two-stage technique first attempts to measure the overall noise in the image and then corrects it by including rich spatial noise based on local bias concerns. Using these complex methodologies, the method attempts to improve the image quality and resolution, which shows its promise in image processing applications where noise reduction and image enhancement are crucial [9].

Both possibilities involve the occurrence of danger and can lead to brain damage or even fatal consequences. Unnecessary strategies have been deliberately used to address this problem. The problems with respiratory sensing systems (RDS) in MRI encryption include PSO, fuzzy C-means (FCM), electromagnetic optimization (EMO), and level set method (LSM). Princes heavily isolated them. The intelligence used in the context of PSO can help in MRI image segmentation, which is known to create several consequences. They demonstrated the adaptability and usefulness of PSO and hybrid algorithms based on swarm intelligence concepts in applications. This necessitates modern computational approaches to solve complex medical image analysis problems, ultimately leading to I am Confident [11].

Fuzzy logic uniquely maps human vision onto colors, allowing clusters to be displayed non-linear and non-rectangularly. With the introduction of fuzzy logic, color representation becomes more complex and reflects human perception. The Comprehensive Learning Particle Swarm Optimization (CLPSO) method outperformed standard algorithms such as Fuzzy C-Means (FCM) and K-Means during testing. This discovery opens up a wider range of real-world applications, demonstrating the efficiency and adaptability of CLPSO in handling complex data clustering jobs with improved performance results. The successful use of CLPSO demonstrates its potential to change approaches to color representation and improve the efficiency of data processing procedures in various industries [12].

Using fuzzy logic for image segmentation of MRI lung data with intensity inhomogeneities marks a significant development in medical imaging analysis. The novel approach entails changing the Fuzzy C-Means (FCM) algorithm's target function so that the surrounding voxels' values impact voxel values. This technique incorporates flexibility and contextuality, allowing for more accurate segmentation of MRI images with significant intensity changes. It is especially remarkable for its ability to segment heavily damaged MRI images, where typical segmentation algorithms may fail to give exact findings. This approach improves the resilience and accuracy of image analysis by combining spatial information and fuzzy logic into the segmentation process, resulting in enhanced diagnostic capabilities and patient care in medical imaging [13].

They investigated the FCM clustering approach in further depth in their study effort. FCM's shortcomings include a partition matrix and random initialization, which causes clustering results to be inconsistent [8]. An alternate approach, Subtractive Clustering (SC), was examined, however the number of clusters was unknown. To alleviate the disadvantages of FCM and SC, the authors presented a novel hybrid approach known as Subtractive Fuzzy C Means (SFCM). The experimental findings show that the SFCM approach generates much superior clustering outcomes than the FCM algorithm indices [14].

The ABC-FCM algorithm is a clustering method that combines the FCM algorithm with the ABC algorithm. It was created to address the limitations of the conventional FCM algorithm, such as initialization sensitivity, local optima, and cluster centroids [15]. The technique takes advantage of the ABC capabilities in the cluster centers, which are then used as input for the FCM algorithm to improve the division preparation of MRI lung images [16].

The EMO algorithm and how to apply it are thoroughly detailed. The EMO approach uses a physics-based attraction-repulsion mechanism to change sample locations to find the optimal answer. The random local search of the EMO algorithm enhances and increases the accuracy of issue resolution [17]. This paper presented a unique technique to local search that utilized and applied the pattern search method in the population shrinking strategy problem. The proposed approach was applied to several problems, and the results were compared to those obtained using the original EMO algorithm [18].

Only a few scholars have solved the Combinatorial Optimization Problem (COP) using the EML approach. This work sought to combine genetic operators with random key concepts to develop a unique hybrid algorithm for obtaining the best/optimal schedule for the problem. When the results of the hybrid algorithm were compared to those of the classic GA and EMO algorithms, they showed higher values [19].

Histogram equalization is a technique used to enhance the contrast of an image by adjusting the intensity levels of its pixels. In this process, the intensity levels are represented by n_k, where the total number of pixels in the image is denoted as N. The fundus image, represented by 'm', consists of pixel intensities ranging from 0 to L-1. The normalized histogram, denoted as ϱ, is calculated by dividing the number of pixels with intensity n by the total number of pixels for each intensity level from 0 to L-1.

$$p = \frac{no.of\ pixcels\ with\ intensity}{total\ no.of\ pixcels}$$

Where L is the intensity values.
P is normalized histogram.
This method helps in improving the visual quality of images by redistributing the intensity values effectively [20].

As a result, the fundus image is enlarged and tends to reach its peak brightness.. Reassigning intensity pixel values to existing ones produces a homogeneous intensity distribution. Histogram equalization increases the contrast of the filtered image.

Firstly, Load the DICOM-formatted MRI respiratory system picture from the scanner.

Secondly, Convert images into main image file formats (.jpeg,.gif,.png,.bmp, etc.).

Thirdly, Save the images with the main .jpeg extensions.

Fourth, Convert the picture to a 3D matrix and read image attributes like size, color, and type.

Fifth, Apply HE to the MRI image and use equation (3.1) f(x,y)= HE∈S_xy {g(s,t)}.

where f(x, y) is the newly calculated pixel value, N x M is the window size, and s x y is the sub-image window coordinates.

Sixth, Save the generated photographs, together with the time of execution, size of memory, and variety in pixels, for future investigation.

Fuzzy logic algorithm (FLA)

Efficient quantitative techniques are crucial in investigations, especially for detecting complex patterns in high-dimensional data. FLA, or Feature Level Fusion, plays a key role in pattern recognition and compression tasks. In design recognition scenarios, images are processed to extract essential features, which are then stored for comparison with new data sets to determine similarities or differences. This method aids in accurate pattern recognition and analysis. FLA is a practical approach to detect optical panels. The localization stage of the proposed study involves the estimation of optics. The sequential method of the FLA algorithm is as follows [21].

The sequential method of the FLA algorithm is as follows.

Firstly: Procedure FLA (image set X, cluster K): X = 〖(X_i)〗_(i=1)^N and K Return U and R.

Secondly, it involves starting nU0 at random.

Thirdly, Repeat.

Fourth, the values are saved between 0 and 1, which explain the membership information focuses for each cluster, while the difficult C-means employments and 1 are the two values for the participation function.

$$J^1(u,v)=\sum_{i=1}^{c}\sum_{j=1}^{n}u_{ij}^{m}\left\|X_j-V_i\right\|^2.$$

Fifth: Implement the equation

$$J^1(u,v)=\sum_{i=1}^{c}\sum_{j=1}^{n}u_{ij}^{m}\left\|X_j-V_i\right\|^2.$$

u is the membership value of J X with concern to cluster i

$$u_{ij}=\frac{1}{\sum_{k=1}^{c}\left(\left\|X_j-V_i\right\|/\left\|X_j-V_k\right\|\right)^{2/(m-1)}}$$

The cluster fuzziness parameter (m: ʿvm„d1ʿw) is set to 2 by default. When images are clustered, each pixel point is considered and included in the clustering process. n represents the number of clusters with a default beginning value larger than one. The FLA algorithm's output argument is the objective function, which explains the parameters below [21].

Sixth, End the operation.

PNN Classifier

Below are the essential layers that were used in the preparation and testing of PNN: Algorithm 1: Classification of Respiratory Detection System using PNN Entry: take respiratory images from the datasets. Outcome: The respiratory images (CI) were classified as unhealthy or healthy. equation CI = Classify (I).

1. Stretch in comparison. Apply the average filter to the image, followed by the sharpening process.
2. Use quadtree-based image fusion techniques to merge contrast and filtered images, as described in Section 3.1.
3. Separate the fused photo collection into training and test sets.
4. Input dataset which already trained (512 x 512 x 1) into the PNN network.
5. The model begins with a 2D CNN layer comprising 96 filters of size [11, 11] and a stride of 4 for feature extraction.
6. A Rectified Linear Unit (ReLU) layer is applied to introduce non-linearity to the network.
7. Subsequently, a max-pooling layer is utilized for spatial down-sampling to retain essential features.
8. Another 2D convolutional layer follows this time with 10 filters of size [5, 5] for further feature extraction.
9. A ReLU layer is applied to introduce non-linearity to the network.
10. A max-pooling layer is used for down-sampling to reduce dimensionality.
11. A fully connected layer with an output size of 512 neurons is employed for feature mapping.
12. A ReLU layer follows to introduce non-linearity to the network.
13. Dropout regularization is applied with a dropout probability to prevent overfitting.
14. Finally, a fully connected layer with an output size of 2 is used for classifying images as unhealthy or healthy.
15. Softmax layer is applied to normalize the output scores into probabilities for classification.
16. The dataset is then classified using a classification layer based on the highest probability output.

3. Results

The PNN algorithm is used to analyze MRI image data using MATLAB (R2020 b) software and produce accurate and timely results for medical purposes. The methodology involves preprocessing, segmentation, and validation.

(1)

(2)

(3)

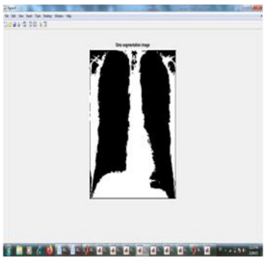

(4)

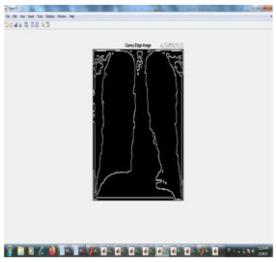

(5)

(6)

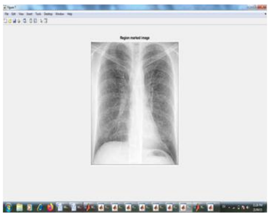

(7)

Figure 1. The experimental message of the simple images

1. Affected system.
2. Histogram Equalization image.
3. Fuzzy C-Means threshed image.
4. Ostu's image.
5. Canny edge detected image. 6- Segmented region image. 7- Labeled Image.

Figure 2. The experimental message of the simple images

1. Affected system.
2. Histogram Equalization image.
3. Fuzzy C-Means threshed image.
4. Ostu's image.
5. Canny edge detected image.
6. Segmented region image.
7. Labeled Image.

(1)

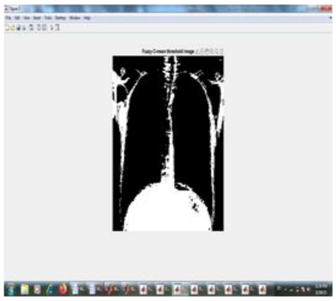

(2)

(3)

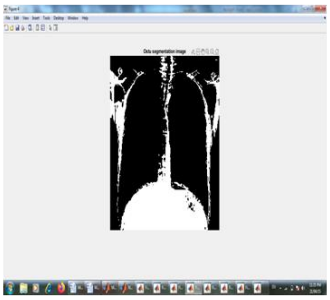

(4)

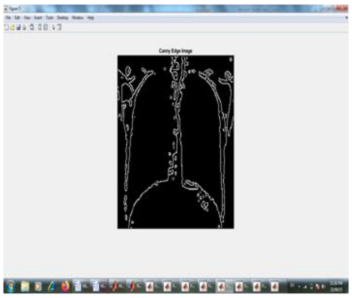

(5)

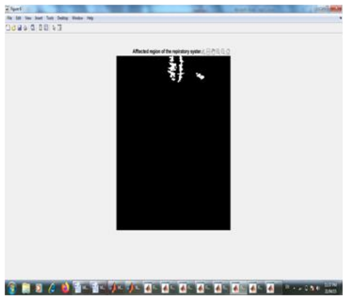

(6)

(7)

Figure 3. The experimental message of the simple images

1. Affected system.
2. Histogram Equalization image
3. Fuzzy C-Means threshed image.
4. Ostu's image.
5. Canny edge detected image.
6. Segmented region image.
7. Labeled Image.

4. Discussion

Table 1. Performance measures of 80 % training and 20% testing of respiratory image 1.

Algorithm	P	TPR	FPR	F-measure	Accuracy(%)
ANN	0.9004	0.8999	0.1	0.89	90
PNN	**0.9903**	**0.9823**	**0.01667**	**0.98**	**98.33**

The normal classification exactness gotten by ANN is 90% as shown in Table 1. In any case, **PNN** gives superior classification comes about as compared to others.

Table 2. Performance measures of 10-fold cross-validation of sample image 1.

Algorithm	P	TPR	FPR	F-measure	Accuracy(%)
ANN	0.95	0.95	0.04	0.95	95.34
PNN	**0.96**	**0.9823**	**0.012**	**0.987**	**98.64**

The normal classification exactness obtained by ANN is 95.34%, as shown in Table 2. In any case, PNN gives a better classification result than other methods.

Table 3: Performance measures of 80 % training and 20% testing of respiratory image 2.

Algorithm	P	TPR	FPR	F-measure	Accuracy(%)
ANN	0.87	0.876	0.060	0.87	87.78
PNN	**0.923**	**0.924**	**0.039**	**0.923**	**92.64**

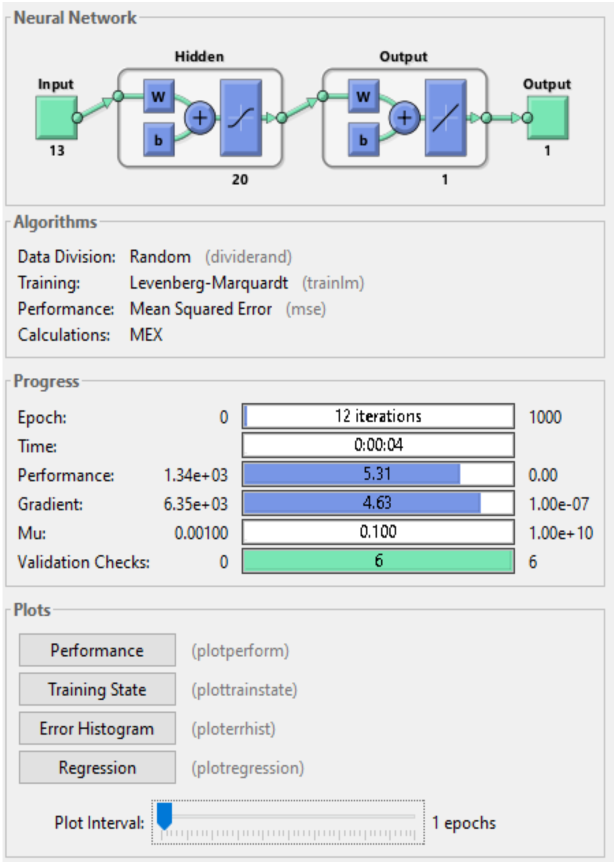

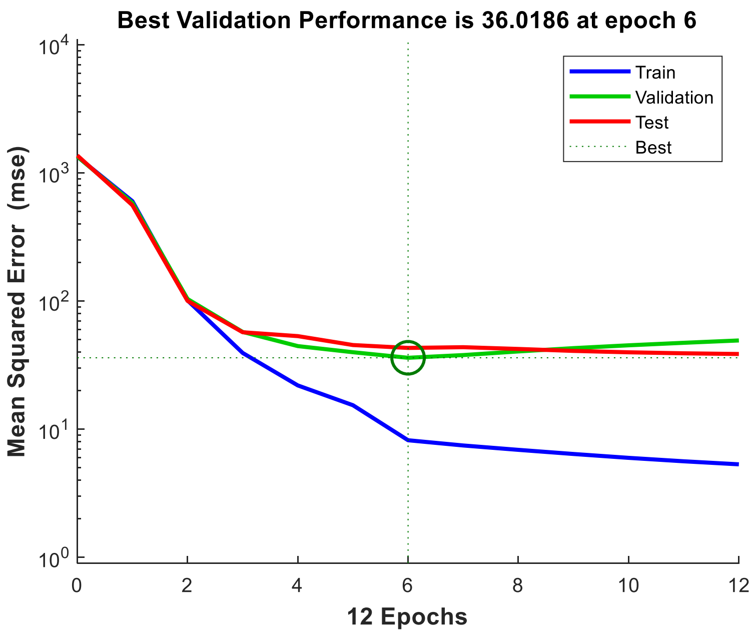

Figure 3. Performance measurements for validation

This graph will not reveal any significant concerns with making ready. The acceptance and test bends are quite comparable.

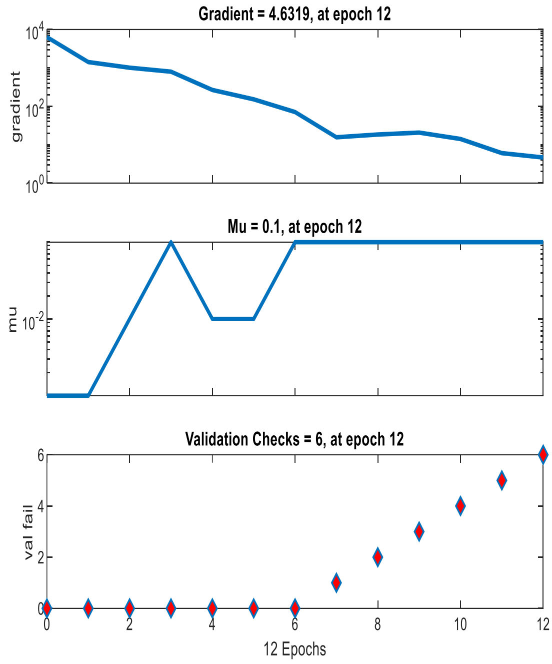

Figure 4. A graph for training a neural network

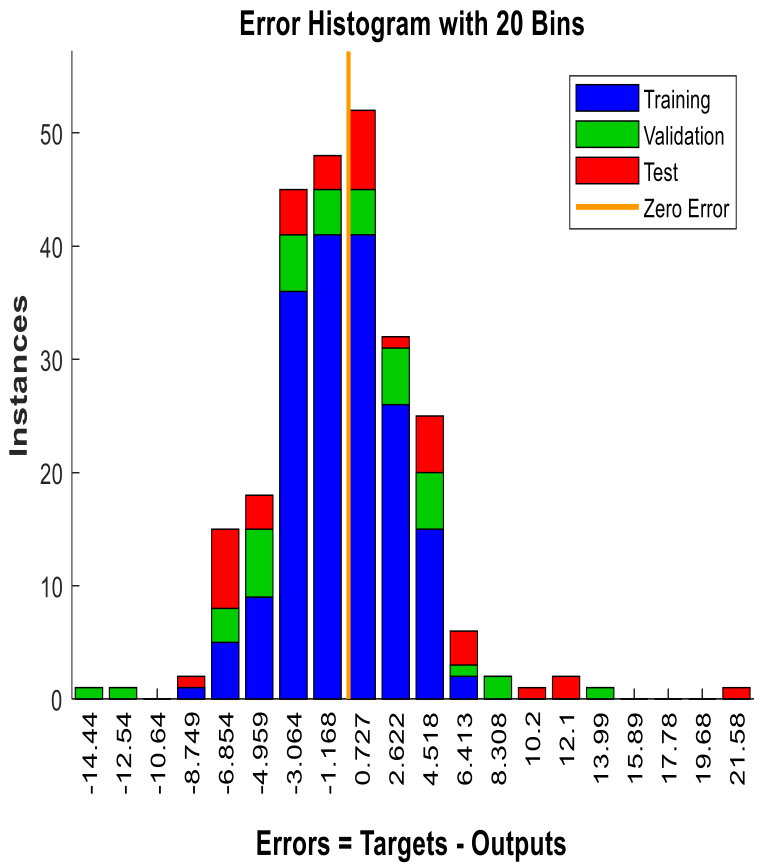

Figure 5. Error graph of histogram

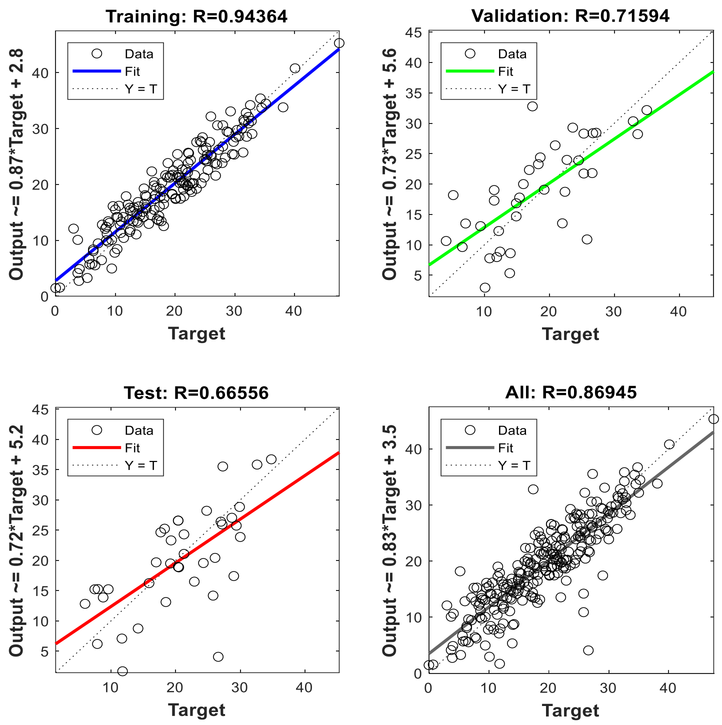

Figure 6. Regression plot for PNN classifier

Figure 7. Visualizes the CNN classification output, the standard metrics for many characteristics. From the table, it is feasible to determine which feature combinations yield more accuracy. Border error represents the frequency of faulty pancreatic pictures. This delivers a higher accuracy of 98.57%.

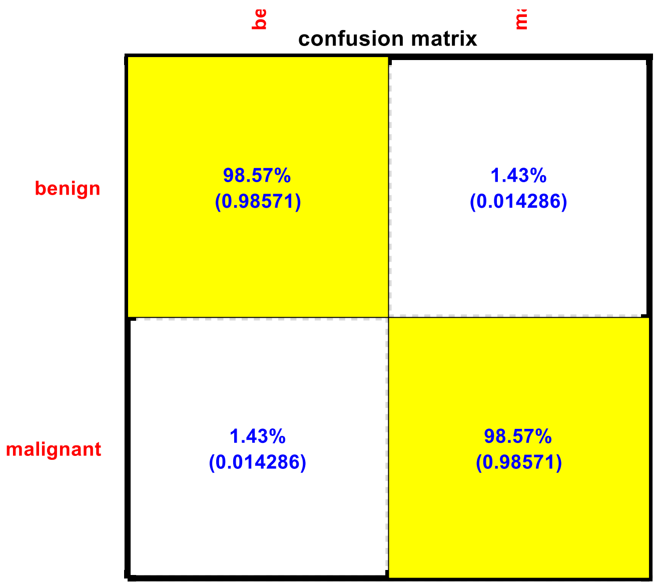

Figure 7. Confusion matrix of CNN classifier

5. Conclusions

This paper presents a PNN classification technique utilizing picture combination and significant learning methodology for the detection of the respiratory system. We have preprocessed the input picture utilizing a quadtree-based picture HE channels strategy. The HE procedure has been utilized to move forward with the separation of the RDS district. After that, a present-day PNN building has been proposed to classify respiratory passing into two (strong and undesirable pictures) and three categories (kind, unsafe, and conventional) from MRI pictures. In this way, it can be particularly unfaltering for the masters inside the event that it is utilized in supportive hone.

REFERENCES

[1] J. C. Bezdek, "Objective Function Clustering," in *Pattern Recognition with Fuzzy Objective Function Algorithms*, Springer US, 1981, pp. 43–93. doi: 10.1007/978-1-4757-0450-1_3.

[2] S.-D. Chen, "A new image quality measure for assessment of histogram equalization-based contrast enhancement techniques," *Digit Signal Process*, vol. 22, no. 4, pp. 640–647, Jul. 2012, doi: 10.1016/j.dsp.2012.04.002.

[3] C. Piewbang, A. Rungsipipat, Y. Poovorawan, and S. Techangamsuwan, "Cross-sectional investigation and risk factor analysis of community-acquired and hospital-associated canine viral infectious respiratory disease complex," *Heliyon*, vol. 5, no. 11, p. e02726, Nov. 2019, doi: 10.1016/j.heliyon.2019.e02726.

[4] V. S. Nallanthighal, Z. Mostaani, A. Härmä, H. Strik, and M. Magimai-Doss, "Deep learning architectures for estimating breathing signal and respiratory parameters from speech recordings," *Neural Networks*, vol. 141, pp. 211–224, Sep. 2021, doi: 10.1016/j.neunet.2021.03.029.

[5] J. J. Feddema and E. Claassen, "Prevalence of viral respiratory infections amongst asthmatics: Results of a meta-regression analysis," *Respir Med*, vol. 173, p. 106020, Nov. 2020, doi: 10.1016/j.rmed.2020.106020.

[6] Y. Zhang *et al.*, "A novel point-of-care test of respiratory syncytial viral RNA based on cellulose-based purification and convective PCR," *Clinica Chimica Acta*, vol. 511, pp. 154–159, Dec. 2020, doi: 10.1016/j.cca.2020.10.012.

[7] J. R. Machado Fernández and L. Anishchenko, "Mental stress detection using bioradar respiratory signals," *Biomed Signal Process Control*, vol. 43, pp. 244–249, May 2018, doi: 10.1016/j.bspc.2018.03.006.

[8] S. S. Sai Koushik and K. G. Srinivasa, "Detection of respiratory diseases from chest X rays using Nesterov accelerated adaptive moment estimation," *Measurement*, vol. 176, p. 109153, May 2021, doi: 10.1016/j.measurement.2021.109153.

[9] M. Abreu, A. Fred, J. Valente, C. Wang, and H. da Silva, "Morphological autoencoders for apnea detection in respiratory gating radiotherapy," *Comput Methods Programs Biomed*, vol. 195, p. 105675, Oct. 2020, doi: 10.1016/j.cmpb.2020.105675.

[10] C. Bi *et al.*, "Simultaneous detection and mutation surveillance of SARS-CoV-2 and multiple respiratory viruses by rapid field-deployable sequencing," *Med*, vol. 2, no. 6, pp. 689-700.e4, Jun. 2021, doi: 10.1016/j.medj.2021.03.015.

[11] B. Jin, Y. Zhao, and Y. Liang, "RETRACTED: Internet of things medical image detection and pediatric renal failure dialysis complicated with respiratory tract infection," *Microprocess Microsyst*, vol. 83, p. 104016, Jun. 2021, doi: 10.1016/j.micpro.2021.104016.

[12] C. Adrover-Jaume *et al.*, "Paper biosensors for detecting elevated IL-6 levels in blood and respiratory samples from COVID-19 patients," *Sens Actuators B Chem*, vol. 330, p. 129333, Mar. 2021, doi: 10.1016/j.snb.2020.129333.

[13] J. Zhang, Z. Yang, Q. Liu, and H. Liang, "Electrochemical biotoxicity detection on a microfluidic paper-based analytical device via cellular respiratory inhibition," *Talanta*, vol. 202, pp. 384–391, Sep. 2019, doi: 10.1016/j.talanta.2019.05.031.

[14] S. Haridy, A. Maged, A. W. Baker, M. Shamsuzzaman, H. Bashir, and M. Xie, "Monitoring scheme for early detection of coronavirus and other respiratory virus outbreaks," *Computers & Industrial Engineering*, vol. 156, p. 107235, Jun. 2021, doi: 10.1016/j.cie.2021.107235.

[15] B. V. Ribeiro, T. A. R. Cordeiro, G. R. e Freitas, L. F. Ferreira, and D. L. Franco, "Biosensors for the detection of respiratory viruses: A review," *Talanta Open*, vol. 2, p. 100007, Dec. 2020, doi: 10.1016/j.talo.2020.100007.

[16] H. G. Lee *et al.*, "PCR-coupled Paper-based Surface-enhanced Raman Scattering (SERS) Sensor for Rapid and Sensitive Detection of Respiratory Bacterial DNA," *Sens Actuators B Chem*, vol. 326, p. 128802, Jan. 2021, doi: 10.1016/j.snb.2020.128802.

[17] Z. Zhao *et al.*, "Advancements in electrochemical biosensing for respiratory virus detection: A review," *TrAC Trends in Analytical Chemistry*, vol. 139, p. 116253, Jun. 2021, doi: 10.1016/j.trac.2021.116253.

[18] E. F. Greneker III, "<title>Radar sensing of heartbeat and respiration at a distance with security applications</title>," in *Radar Sensor Technology II*, R. Trebits and J. L. Kurtz, Eds., SPIE, Jun. 1997, pp. 22–27. doi: 10.1117/12.276106.

[19] M. Cao, Q. Sun, X. Zhang, Y. Ma, and J. Wang, "Detection and differentiation of respiratory syncytial virus subgroups A and B with colorimetric toehold switch sensors in a paper-based cell-free system," *Biosens Bioelectron*, vol. 182, p. 113173, Jun. 2021, doi: 10.1016/j.bios.2021.113173.

[20] L. Chen, M. Hu, N. Liu, G. Zhai, and S. X. Yang, "Collaborative use of RGB and thermal imaging for remote breathing rate measurement under realistic conditions," *Infrared Physics & Technology*, vol. 111, p. 103504, Dec. 2020, doi: 10.1016/j.infrared.2020.103504.

[21] P. Viola and M. Jones, "Rapid object detection using a boosted cascade of simple features," in *Proceedings of the 2001 IEEE Computer Society Conference on Computer Vision and Pattern Recognition. CVPR 2001*, in CVPR-01, vol. 1. IEEE Comput. Soc, pp. I-511–I-518. doi: 10.1109/cvpr.2001.990517.